Nuclear Medicine and Biology 39 (2012) 1213–1218

Contents lists available at SciVerse ScienceDirect

Nuclear Medicine and Biology

journal homepage: www.elsevier.com/locate/nucmedbio

Transport mechanism of ^{11}C-labeled L- and D-methionine in human-derived tumor cells☆,☆☆

Masato Kobayashi [a,b,1], Fumiya Hashimoto [a,1], Kazuyo Ohe [a], Takahiro Nadamura [a], Kodai Nishi [a], Naoto Shikano [c], Ryuichi Nishii [d], Tatsuya Higashi [e], Hidehiko Okazawa [b], Keiichi Kawai [a,b,*]

[a] School of Health Sciences, College of Medical, Pharmaceutical and Health Sciences, Kanazawa University, Kanazawa 920-0942, Japan
[b] Biomedical Imaging Research Center, University of Fukui, Fukui 910-1193, Japan
[c] Department of Radiological Sciences, Ibaraki Prefectural University of Health Sciences, Ibaraki 300-0331, Japan
[d] Department of Radiology, School of Medicine, Miyazaki University, Miyazaki 889-2192, Japan
[e] Division of PET Imaging, Shiga Medical Center Research Institute, Shiga 524-8524, Japan

ARTICLE INFO

Article history:
Received 25 April 2012
Received in revised form 19 May 2012
Accepted 7 June 2012

Keywords:
Methionine
PET
Tumor
Amino acid transport system
Gene expression

ABSTRACT

Introduction: *S*-methyl-^{11}C-labeled L- and D-methionine (^{11}C-L- and D-MET) are useful as radiotracers for tumor imaging. However, it is not known whether the transport mechanism of ^{11}C-D-MET is the same as that for ^{11}C-L-MET, which is transported by the amino acid transport system L. In this study, we investigated the transport mechanism of ^{11}C-L- and D-MET by analyzing the expression of transport system genes in human-derived tumor cells.

Methods: The expression of transport system genes in human-derived tumor cells was quantitatively analyzed. The mechanism of MET transport in these cells was investigated by incubating the cells with [*S*-methyl-^{3}H]-L-MET (^{3}H-L-MET) or [*S*-methyl-^{3}H]-D-MET (^{3}H-D-MET) and the effect of 2-amino-2- norbornane-carboxylic acid, a system L transport inhibitor, or α-(methylamino)isobutyric acid, a system A transport inhibitor, on their transport was measured. The transport and metabolic stability of [*S*-methyl-^{14}C]-L-MET (^{14}C-L-MET) and ^{3}H-D-MET was also analyzed using bearing mice with H441 or PC14 tumor cells.

Results: ^{3}H-D-MET was mainly transported by both systems L and alanine–serine–cysteine (ASC), while system L was involved in ^{3}H-L-MET transport. There was a high correlation between both ^{3}H-L-MET and ^{3}H-D-MET uptake and the expression of amino acid transport system genes. In the in vivo study, H441-cell accumulation of ^{3}H-D-MET was higher than that of ^{14}C-L-MET. Hepatic and renal accumulation of ^{3}H-D-MET was lower than that of ^{14}C-L-MET.

Conclusion: The transport mechanism of ^{3}H-D-MET was different from that of ^{3}H-L-MET. Since ^{3}H-D-MET has high metabolic stability, its accumulation reflects the transporter function of system L and ASC.

1. Introduction

Amino acid transporter genes are highly expressed in tumor cells and enable these cells to take up a large amount of amino acids [1]. These transporters are categorized into at least 17 distinct classes [2]. Neutral amino acids are considered to be mainly transported by three systems: systems L, A, and alanine–serine–cysteine (ASC) [3]. [*S*-methyl-^{11}C]-L-methionine (^{11}C-L-MET), a natural amino acid, has been used as a positron emission tomography (PET) tracer to detect tumors. ^{11}C-L-MET is transported into cells via the amino acid transport system L. ^{11}C-L-MET accumulates in tumors due to the enhanced protein synthesis and transmethylation metabolic functions of tumors that allow ^{11}C-L-MET to become incorporated into the tumor molecules [4]. In a clinical study, ^{11}C-L-MET has been used in the diagnosis and follow-up of glioma patients and is superior to 2-^{18}F-fluoro-2-deoxy-D-glucose (^{18}F-FDG) for delineating tumor margins [5,6]. In addition, there are reports that ^{11}C-L-MET is as useful as ^{18}F-FDG in the differential diagnosis of lung cancer [7]. Currently, there are limitations to the use of ^{18}F-FDG for the diagnosis of cerebral tumors because ^{18}F-FDG also accumulates in normal brain tissue. Furthermore, ^{11}C-L-MET cannot be applied to the detection of abdominal tumors because it accumulates in metabolically normal tissues and is affected by enzymatic metabolism.

D-methionine (D-MET) is considered to be less affected by enzymatic metabolism than L-MET. Since there is very little metabolism of [*S*-methyl-^{11}C]-labeled D-MET (^{11}C-D-MET), ^{11}C-D-MET has

☆ Conflicts of interest: There are no conflicts of interest.

☆☆ Financial support: This study was partly funded by Grants-in-Aid for Scientific Research from the Japan Society for the Promotion of Science (Nos. 21659268, 22591372, 22791180, and 23300361).

* Corresponding author. Tel.: +81 76 265 2527; fax: +81 76 234 4366.
E-mail address: kei@mhs.mp.kanazawa-u.ac.jp (K. Kawai).

[1] Masato Kobayashi and Fumiya Hashimoto are co-first authors and contributed equally to this work.

0969-8051/$ – see front matter © 2012 Elsevier Inc. All rights reserved.
http://dx.doi.org/10.1016/j.nucmedbio.2012.06.006

been suggested as a potentially useful PET tracer for tumor imaging [8–10]. According to Tsukada et al. [10], who evaluated ^{11}C-D-MET accumulation using human cervical carcinoma-derived HeLa cells, the accumulation of ^{11}C-D-MET in tumors is superior to that of ^{11}C-L-MET. However, the transport mechanism by which ^{11}C-D-MET accumulates in tumors has not been identified. In this study, we determined the mechanism of accumulation of ^{11}C-D-MET and reinvestigated the mechanism of ^{11}C-L-MET accumulation in human-derived tumor cells. Because ^{11}C-L-MET has a short half-life, *S*-methyl-^{3}H or *S*-methyl-^{14}C, both of which act in the same way as ^{11}C-L-MET, was used instead of ^{11}C-L-MET. Real-time reverse transcription-polymerase chain reaction (qRT-PCR) was used to measure the gene expression of neutral amino acid transport systems. Correlations between tumor accumulation of L-MET and D-MET and the gene expression of neutral amino acid transport systems were evaluated in an in vitro study. In addition, since the stability of L-MET and D-MET in normal tissue has not been thoroughly investigated, the metabolic stability of L-MET and D-MET was assessed in the mouse liver and kidney, which are responsible for their metabolism.

2. Materials and methods

2.1. Materials

[*S*-methyl-^{3}H]-L-methionine (^{3}H-L-MET: 2.96 GBq/mmol), [*S*-methyl-^{3}H]-D-methionine (^{3}H-D-MET: 2.96 GBq/mmol), [*S*-methyl-^{14}C]-L-MET (^{14}C-L-MET: 2.22 GBq/mmol) and [*S*-methyl-^{14}C]-D-MET (^{14}C-D-MET: 2.22 GBq/mmol) were purchased from American Radiolabeled Chemicals Co. (St. Louis, MO, USA).

2.2. Tumor cells

The cultured human tumor cell lines H441, PC14 and MDA-MB435 were got from the University of Texas, MD Anderson Cancer Center, Houston, TX, USA. The LS180 cell line was purchased from Dainippon Sumitomo Pharma Co., Ltd (Osaka, Japan). H441 and PC14 are pulmonary adenocarcinoma cell lines, MDA-MB435 is a breast cancer cell line and LS180 is a colon cancer cell line. These cancer cells were selected as representative cells to evaluate transport mechanism of L- and D-MET. All tumor cells (2.0×10^5 cells/ml/well) were incubated in 24-well plates with 2 ml of Dulbecco's modified Eagle's medium (pH 7.4; Sigma Chemical Co., St. Louis, MO, USA) in a 10% CO_2 atmosphere. A cell proliferation curve was prepared to determine the duration of the logarithmic growth phase.

2.3. qRT-PCR analysis of human-derived tumor cells

Total RNA was harvested from each tumor cell using an RNeasy Mini kit (QIAGEN K. K, Tokyo, Japan). The quality of the total RNA was evaluated using a bioanalyzer (Agilent Technologies, Santa Clara, CA, USA). Complementary DNA (cDNA) was amplified only from high-quality total RNA using an AffinityScript qRT-PCR cDNA Synthesis kit (Agilent Technologies). The thermal profile of the reaction was as follows: 5 min at 25°C for 1 cycle, 15 min at 42°C for 1 cycle and 55 min at 95°C for 1 cycle. The genes analyzed by qRT-PCR were Na^+-dependent transport systems A (SNAT1, SNAT2, SNAT4) and ASC (ASCT1, ASCT2), and Na^+-independent transport systems L (LAT1, LAT2, LAT3, LAT4) and 4F2hc. Two different housekeeping genes, glyceraldehyde-3-phosphate dehydrogenase (GAPDH) and beta actin (ACTB) were used as internal controls to compensate for the differences between the initial RNA and cDNA amounts. An Mx3005P thermocycler (Agilent Technologies) was used for the qRT-PCR reactions. Primers were synthesized by Nihon Gene Research Laboratories, Inc. (Miyagi, Japan). The artificial plasmid used for the calibration curve was synthesized by GenScript (Piscataway, NJ, USA). The qRT-PCR reagent used in this study was Brilliant II Fast SYBR Green qRT-PCR Master Mix (Stratagene Products Division, Agilent Technologies). The thermal profile of the reaction was as follows: 2 min at 95°C for 1 cycle, 5 s at 95°C followed by 20 s at 60°C for 40 cycles, 1 min at 95°C followed by 30 s at 55°C and 30 s at 95°C for 1 cycle. In addition, serial dilutions of artificial plasmids were performed. The samples used were created using a dilution series ranging from 1×10^2 to 1×10^8 copies per tube for the calibration curve. All reactions were performed in triplicate.

2.4. Assay of MET transport in human-derived tumor cells

Transport assays were performed according to the method developed by Shikano et al. [11]. In brief, tumor cells were seeded on 24-well cell culture multiwell plates at a density of 2×10^5 cells/ml/well. The assays were conducted 24 h after seeding.

The sodium-containing incubation medium used was based on phosphate-buffered saline (Na^+-PBS), consisting of 137 mM NaCl, 2.7 mM KCl, 8 mM Na_2HPO_4, 1.5 mM KH_2PO_4, 5.6 mM D-glucose, 0.9 mM $CaCl_2$ and 0.5 mM $MgCl_2$. In the sodium-free incubation medium (Na^+-free PBS), NaCl and Na_2HPO_4 were replaced with the equivalent concentration of choline chloride and K_2HPO_4, respectively. After the culture medium was removed, each well was incubated with 1 ml of incubation medium for 10 min at 37°C. The cells were then incubated with 0.5 ml of incubation medium containing the ^{3}H-L-MET or ^{3}H-D-MET (18.5 kBq) for 0.5 min at 37°C as a control condition. For the competitive inhibition assay, the cells were incubated with ^{3}H-L-MET or ^{3}H-D-MET and 1.0 mM of inhibitors, 2-amino-2-norbornane-carboxylic acid (BCH; Sigma Chemical Co.), a substrate specific to system L transporters, and α-(methylamino)isobutyric acid (MeAIB; Sigma Chemical Co.), a substrate specific to system A transporters. At the end of the incubation, each well was rapidly washed twice with 1 ml of ice-cold incubation medium. The cells were then solubilized in 0.5 ml of 0.1 N NaOH, mixed with an ASC-II Scintillation Cocktail (GE Healthcare UK Ltd, Little Chalfont, England), and radioactivity was then measured with a liquid scintillation counter (Aloka, Tokyo, Japan; LSC-5100). Subsequently, the cells were detached from one another with trypsin to facilitate further counting. All experimental conditions were examined in quadruple assays. Reproducibility was confirmed by repeating the same experiment.

To measure the contribution of amino acid transport systems to MET transport, we used the method devised by Shotwell [12] and Nakajima et al. (Fig. 1) [13]. Briefly, MET uptake in the absence of inhibitors was calculated as a percentage of the control value, which was set at 100%. System A transport was calculated by subtracting MET uptake in the presence of MeAIB from uptake in the control Na^+-PBS. System ASC transport was calculated by subtracting the value of MET uptake in control Na^+-free PBS from MET uptake in the presence of MeAIB. Finally, system L participation was calculated by subtracting MET uptake in the presence of BCH from MET uptake in control Na^+-free PBS. The rates of tumor uptake of ^{3}H-L-MET and ^{3}H-D-MET were calculated as uptake rates per 10^5 tumor cells (% injected dose (ID)/10^5 cells). The correlation between tumor uptake of ^{3}H-L-MET and ^{3}H-D-MET and expression of neutral amino acid transport system genes was also examined. The result for each set of experimental conditions represents the mean of four wells on the cell culture multiwell plates.

2.5. Biodistribution of ^{14}C-L-MET and ^{3}H-D-MET in tumor-bearing mice

Animal studies were approved by the Animal Care Committee at Kanazawa University and were conducted in accordance with the international standards for animal welfare and institutional guidelines. Adequate measures were taken to minimize pain and discomfort. Male KSN/Slc nude mice from Japan SLC Inc. (Hamamatsu, Japan) were housed for 1 week under a 12-h light/12-h dark cycle with free access to food and water. The mice were fasted with no food overnight with water supplied ad libitum before experiments.

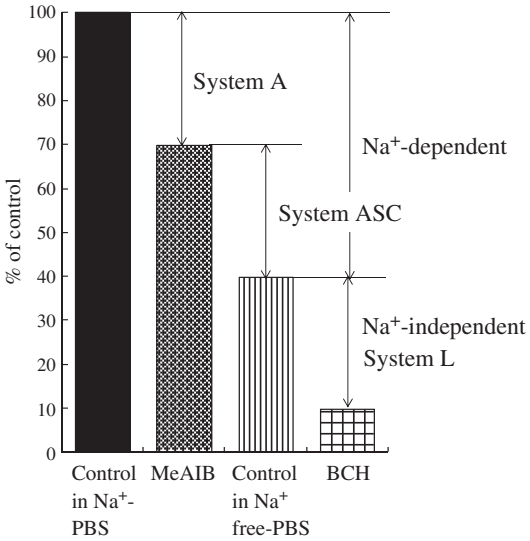

Fig. 1. Calculation of the contribution of amino acid transport systems to MET uptake. 100%=control uptake of ^{3}H-L-MET or ^{3}H-D-MET in Na^{+}-PBS. System A=(control uptake of ^{3}H-L-MET or ^{3}H-D-MET in Na^{+}-PBS)−(uptake of ^{3}H-D-MET or ^{3}H-L-MET with MeAIB inhibitor in Na^{+}-PBS). System ASC=(uptake of ^{3}H-D-MET or ^{3}H-L-MET with MeAIB inhibitor in Na^{+}-PBS)−(control uptake with Na^{+} free-PBS). System L=(control uptake of ^{3}H-L-MET or ^{3}H-D-MET in Na^{+} free-PBS)−(uptake of ^{3}H-L-MET or ^{3}H-D-MET with BCH inhibitor in Na^{+} free-PBS).

H441 cells, in which neutral amino acid transport systems are highly expressed, and PC14 cells, which have the lowest level of expression of amino acid transport systems of the cells assayed in the present study, were prepared to a final density of 2×10^{6} cells per 100 μl. The prepared H441 and PC14 cells (100 μl per mouse) were subsequently injected subcutaneously into the left and right thighs, respectively, of five KSN/Slc nude mice. Approximately 1 week after transplantation of the H441 and PC14 cells, ^{14}C-L-MET (18.5 kBq) and ^{3}H-D-MET (92.5 kBq) were simultaneously injected as double tracers into the tail veins of the tumor-bearing mice. The mice were sacrificed at 2, 10, 30 or 60 min postinjection. After blood was sampled via cardiocentesis, the tumors, pancreas, kidney, muscle and liver were excised. Approximately 100 mg of each excised organ was weighed, and SOLVABLE (Perkin-Elmer, Waltham, MA, USA) was added. The samples were then shaken for ^{3}H at 50°C. After the samples were dissolved, Ultima Gold (Perkin-Elmer) was added. Sample radioactivity was measured using a liquid scintillation counter, and a quenching correction was performed. To compare the accumulation of ^{14}C-L-MET and ^{3}H-D-MET in organs and tumors, the unit of each organ and tumor accumulation was calculated as the percentage of ID per gram (%ID/g). We also evaluated the level of MET accumulated in the tumor relative to that accumulated in each organ by dividing the amount of MET accumulated in H441 or PC14 tumor cells by the amount of MET accumulated in the muscle, liver and plasma of the corresponding tumor-bearing mice. These values are shown as H441 or PC14/muscle, liver or plasma in Table 2.

We also analyzed the levels of ^{14}C-L-MET or ^{3}H-D-MET metabolites in hepatic and renal samples from the tumor-bearing mice. These tissue samples were homogenized in a bicarbonate buffer, and 100% trichloroacetic acid (Nacalai Tesque, Kyoto, Japan) was then added to the homogenate to a final concentration of 5% and mixed. The precipitated fraction was collected in a glass filter (ADVANTEC, Tokyo, Japan) and washed with ice-cold 5% trichloroacetic acid. Protein in the precipitated fraction was fixed using thermal processing at 150°C for 1 h. Radioactivity was measured and was used to evaluate the uptake of ^{14}C-L-MET or ^{3}H-D-MET into the protein fraction. In a further experiment, 18.5 kBq of ^{14}C-L-MET or ^{14}C-D-MET was injected into five normal mice to evaluate the metabolic stability of hepatic and renal samples in the acid-soluble fraction. Because ^{3}H-D-MET will not be appropriated in thin-layer chromatography, ^{14}C-D-MET was used instead as it has the same labeling position and similar uptake properties as ^{3}H-D-MET. Tissue homogenates to which trichloroacetic acid had been added were centrifuged. The supernatant was spotted on a thin-layer chromatography plate, and the signal was then expanded using a developing solvent (butanol/acetic acid/water, 4:1:1) followed by exposure on an imaging plate (BAS-SR 2025; Fuji Film, Tokyo, Japan). BAS5000 (Fuji Film) was then used to evaluate the amount of unmetabolized ^{14}C-L-MET or ^{14}C-D-MET in the acid-soluble fraction. The amount of ^{14}C-L-MET or ^{14}C-D-MET that was metabolized was determined by calculating the rate of ^{14}C-L-MET or ^{14}C-D-MET uptake into protein fractions and the level of the parent ^{14}C-L-MET and ^{14}C-D-MET component.

2.6. Statistical analysis

Data are presented as means and standard deviations (S.D.s). *P* values were calculated using a two-tailed paired Student's *t* test for comparison between two groups. A *P* value less than 0.01 and 0.05 was considered significant.

3. Results

3.1. Gene expression of amino acid transport systems in human-derived tumor cells

The expression of amino acid transport system genes in the human-derived tumor cell lines H441, MDA-MB435, LS180 and PC14 was analyzed using qRT-PCR. The high quality of the total RNA harvested from each tumor cell was confirmed using a bioanalyzer (data not shown). The gene expression levels of neutral amino acid transport systems in each cell line were calculated using a calibration curve for each gene (Table 1). Transporters of the Na^{+}-dependent transport system, system A and system ASC were expressed (in order from the highest to the lowest levels of expression) in H441, MDA-MB435, LS180 and PC14 cells. Transporters of the Na^{+}-independent transport system, system L and the coupling factor, 4F2hc, were highly expressed in H441 cells, followed by MDA-MB435, and then LS180 cells, but little expression was observed in PC14 cells.

3.2. Assay of MET transport in human-derived tumor cells

The contribution of each amino acid transport system to tumor cell uptake of ^{3}H-L-MET and ^{3}H-D-MET was analyzed using specific inhibitors and measured at 0.5 min after ^{3}H-L-MET or ^{3}H-D-MET injection (Fig. 2). System L was involved in tumor uptake of ^{3}H-L-MET and mediated over 50% of the total uptake of ^{3}H-L-MET that was

Table 1
Expression of genes of neutral amino acid transport systems in human-derived tumor cells.

	System	Family	H441	MDA-MB435	LS180	PC14
Na^{+}-dependent	A	SNAT1	91.66	321.56	91.49	76.71
		SNAT2	30.55	127.84	20.34	81.41
		SNAT4	0.02	0.63	0.38	0.01
	ASC	ASCT1	23.6	30.6	8.27	3.35
		ASCT2	65.95	323.37	89.33	29.98
Na^{+}-independent	L	LAT1	568.83	167.93	76.83	6.35
		LAT2	17.87	ND	11.1	ND
		LAT3	0.62	3.66	5.08	0.73
		LAT4	0.80	1.45	3.69	0.24
	Coupling factor	4F2hc	1008.52	608.77	217.08	50.80

Data are expressed as copy number per 1000 copies of housekeeping genes. ND: not determined.

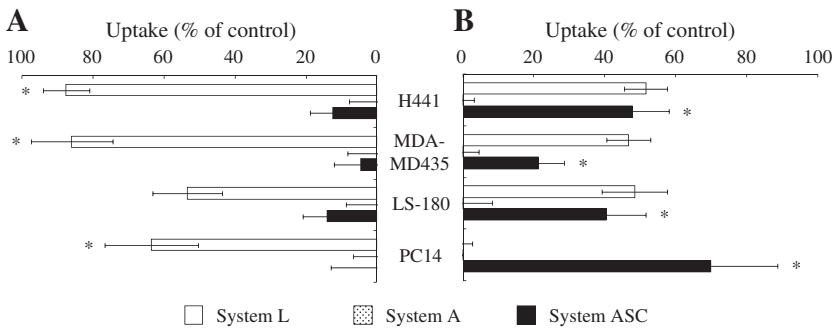

Fig. 2. Contribution of each amino acid transport system to ^{3}H-L-MET and ^{3}H-D-MET uptake in human-derived tumor cells. Tumor uptake at 0.5 min after ^{3}H-L-MET (A) and ^{3}H-D-MET (B) addition is shown. System L played a significant role in tumor transport of ^{3}H-L-MET, whereas both systems L and ASC played a large role in tumor transport of ^{3}H-D-MET, significantly PC14 cells. The asterisks indicate $P<0.01$ between the uptake of ^{3}H-L-MET and ^{3}H-D-MET in each tumor cell.

observed in each of the control tumor cells. System L was also involved in tumor uptake of ^{3}H-D-MET and mediated over 46% of the total ^{3}H-D-MET uptake that was observed in control H441, MDA-MB435 and LS180 cells. However, in PC14 cells, system ASC mediated about 70% of the total ^{3}H-D-MET uptake. System A was not involved in tumor uptake of ^{3}H-L-MET or ^{3}H-D-MET.

3.3. Correlation between MET uptake and transporter gene expression in human-derived tumor cells

The correlation between tumor uptake of MET and the expression of amino acid transport system genes is shown in Fig. 3. The above data (Fig. 2) showed that transport system L was the main mediator of ^{3}H-L-MET transport and that both system L and ASC mediated ^{3}H-D-MET transport. We therefore evaluated correlations between tumor uptake of ^{3}H-L-MET and expression of system L genes, and between tumor uptake of ^{3}H-D-MET and expression of both system L and ASC genes. There was a high correlation between both ^{3}H-D-MET and ^{3}H-L-MET uptake and the expression of amino acid transport system genes.

3.4. Biodistribution of ^{14}C-L-MET and ^{3}H-D-MET in tumor-bearing mice

The biodistribution of ^{14}C-L-MET and ^{3}H-D-MET in H441 and PC14 tumor-bearing mice is shown in Table 2. Tumor accumulation of ^{3}H-D-MET was significantly greater than that of ^{14}C-L-MET in H441-bearing mice. Tumor accumulation of ^{14}C-L-MET and ^{3}H-D-MET in PC14-bearing mice was significantly lower than that of H441-bearing mice. Furthermore, ^{3}H-D-MET accumulation in the PC14 tumors was significantly lower than that of ^{14}C-L-MET. There was high accumulation of both ^{14}C-L-MET and ^{3}H-D-MET in the pancreas and kidney of the tumor-bearing mice, but ^{3}H-D-MET accumulated to a higher level than ^{14}C-L-MET at early time points after injection. The accumulation of ^{3}H-D-MET was lower than that of ^{14}C-L-MET in the liver, but higher in plasma of the tumor-bearing mice.

Fig. 4 shows the percentage of the injected ^{14}C-L-MET and ^{14}C-D-MET incorporated into proteins and nonproteins and the percentage of nonmetabolized ^{14}C-L-MET and ^{14}C-D-MET in the liver (A) and kidney (B) of normal mice at 10 min after injection. Approximately 25% to 50% of the injected ^{14}C-L-MET was incorporated into protein, whereas the level of ^{14}C-D-MET incorporation was much lower at approximately 3%. The incorporation of ^{3}H-D-MET into nonprotein molecules was lower than that of ^{14}C-L-MET. Approximately 20% to 40% of ^{14}C-L-MET, but more than 80% of ^{14}C-D-MET, remained unincorporated.

4. Discussion

In this study, we propose a transport mechanism of MET, particularly of D-MET, into human-derived tumor cells that is based on accurate qRT-PCR evaluation of the gene expression levels of neutral amino acid transport systems in tumor cells. We reconfirmed previous reports [12,14–16] demonstrating that system L was the main system for transport of ^{3}H-L-MET (Figs. 2A and 3A). Shotwell et al. [12] divided the uptake of L-MET by Chinese hamster ovary (CHO)-K1 cells into four components: approximately 52% by system L, 21% by system ASC, 20% by nonsaturable processes and 7% by system A. Oxender and Chistensen [14] reported the involvement of systems L and A in the uptake of ^{14}C-L-MET by Ehrlich cells. Guerino and Baumrucker [15] estimated that ^{14}C-L-MET was transported into cattle small intestine as follows: 54% through system L, 28% through system ASC, 25% through nonsaturable

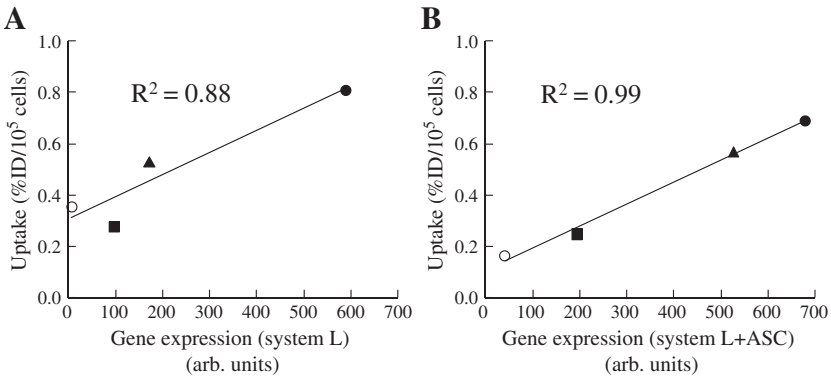

Fig. 3. Correlation between tumor uptake of ^{3}H-L-MET and ^{3}H-D-MET at 0.5 min after the addition and the expression of amino acid transport system genes in human-derived tumor cells. The figures show the relationship between ^{3}H-L-MET uptake and expression of system L genes (A) and that between ^{3}H-D-MET uptakes and expression of system L and ASC genes (B). Cell lines analyzed were as follows: H441 (●), MDA-MB435 (▲), LS180 (■) and PC14 (○). The tumor uptake of ^{3}H-D-MET showed a higher correlation with expression of transport genes than that of ^{3}H-L-MET.

Table 2
Biodistribution of ^{14}C-L-MET and ^{3}H-D-MET in H441 and PC14 tumor-bearing mice.

^{14}C-L-MET					^{3}H-D-MET			
min	2	10	30	60	2	10	30	60
H441	3.94±0.84	7.02±0.75	7.42±1.27	5.46±0.69	4.56±0.65**	11.03±1.52*	13.50±1.98*	10.20±1.09*
PC14	1.24±0.38	3.24±0.45	3.90±0.71	3.15±0.58	1.15±0.25	1.84±0.21*	2.11±0.35*	1.73±0.39*
Pancreas	29.53±2.32	45.60±3.61	43.13±5.96	32.79±7.01	30.61±2.53	57.56±5.17*	26.51±6.08*	10.20±1.09*
Kidney	11.99±0.99	12.62±1.73	8.50±0.87	6.52±0.73	32.83±2.90*	30.70±3.55*	13.86±0.38*	7.20±0.12**
Muscle	2.24±0.13	2.50±0.38	1.68±0.20	1.30±0.21	2.03±0.24	2.33±0.63	1.94±0.21**	1.82±0.33*
Liver	6.21±0.78	10.23±2.11	10.42±1.48	8.13±0.84	3.40±0.32*	3.52±0.44*	2.62±0.19*	1.83±0.12*
Plasma	4.31±0.34	1.94±0.07	1.31±0.09	1.02±0.14	8.26±1.16*	4.76±0.26*	2.44±0.18*	1.45±0.08**
H441/muscle	1.76±0.41	2.81±0.48	4.42±0.56	4.20±0.35	2.25±0.39**	4.73±0.58*	6.96±0.50*	5.60±0.25*
H441/liver	0.63±0.11	0.69±0.13	0.71±0.18	0.67±0.10	1.34±0.18*	3.13±0.41*	5.15±0.43*	5.57±0.18*
H441/plasma	0.91±0.22	3.62±0.10	5.66±0.19	5.35±0.15	0.55±0.15*	2.32±0.27**	5.53±0.49	7.03±0.32*
PC14/muscle	0.55±0.11	1.30±0.25	2.32±0.42	2.42±0.24	0.57±0.22	0.79±0.21**	1.09±0.18*	0.95±0.06*
PC14/liver	0.20±0.11	0.32±0.08	0.37±0.13	0.39±0.47	0.34±0.15**	0.52±0.13*	0.81±0.10*	0.95±0.05*
PC14/plasma	0.29±0.08	1.67±0.31	2.98±0.15	3.09±0.11	0.14±0.07**	0.39±0.10*	0.86±0.09*	1.19±0.04*

Data are expressed as means±.S.D. Values of ^{3}H-D-MET are significantly different than those of ^{14}C-L-MET at each time point after injection (*P<0.01, **P<0.05, paired t test). The units are the percentage of injected dose per gram (%ID/g) of MET accumulated in the tumor cells and in each organ. The values of H441(PC14)/muscle, H441(PC14)/liver and H441(PC14)/plasma indicate the values for MET accumulation in the tumor tissue, divided by MET accumulation in the indicated organ of the corresponding tumor-bearing mice.

processes and 15% through system A. Shikano et al. [16] reported that system L mediated approximately 85% of [1-^{14}C]-labeled L-MET transport in CHO-K1 cells, system A mediated approximately 10% of its intracellular transport and nonsaturable processes mediated approximately 5% of its transport. In contrast to all of these studies that evaluated L-MET transport mechanisms of normal cells expressing specific levels of amino acid transport system genes, our study estimated the L-MET transport mechanism using four different tumor cell lines, which express different levels of transport system genes. The high correlation between tumor uptake of ^{3}H-L-MET and the expression levels of system L genes (R^2=0.88; Fig. 3A) indicated that ^{3}H-L-MET is mainly transported through system L in the tumor cells.

Regarding ^{3}H-D-MET transport, system L was very much involved in its transport in H441, MDA-MB435 and LS180 cells, but system ASC was dominant for its transport in PC14 cells (Fig. 2B). There was a stronger correlation between ^{3}H-D-MET uptake and the expression of system L and ASC genes in the tumor cells than that between ^{3}H-L-MET uptake and the expression of system L genes (R^2=0.99) (Fig. 3). Shikano et al. [16] reported that system L mediated approximately 95% of the transport of [1-^{14}C] labeled D-MET in CHO-K1 cells and that system A mediated approximately 5% of its intracellular transport. Since the labeling position of ^{14}C on D-MET used in their study, [1-^{14}C], differed from that of ^{3}H and ^{11}C used in our study and in clinical studies, [*S*-methyl-^{3}H and ^{11}C], it is important to investigate the transport mechanism of ^{3}H-D-MET based on the gene expression of reporters in various kinds of tumor cells. In our study, the tumor transport of ^{3}H-D-MET was associated with both systems L and ASC (Figs. 2B and 3B). Although we used three different human tumor cell lines — lung, breast and colon cancers — to investigate the transport mechanism of L- and D-MET, the transport mechanism and uptake of MET may be different in the brain tumor cells, which is useful for clinical PET study.

Recent nuclear medicine studies have evaluated the correlation between the uptake of radiotracers and the expression of transport system genes in tumor cells [17–19]. These studies were performed in order to identify the uptake mechanisms of radiotracers in tumor cells. Forstner et al. [17] reported that the imaging results obtained with the three radiotracers, ^{18}F-FDG, 3-deoxy-3-^{18}F-fluorothymidine and ^{18}F-fluoroethylcholine, could be explained by the gene expression patterns of membrane transporters and enzymes that are involved in radiotracer uptake and retention, which were measured in the tumor cells using qRT-PCR. By comparing ^{18}F-FDG PET imaging with the results of qRT-PCR analysis of gene expression, Christen et al. [18] showed that human visceral adipose tissue has increased glucose uptake compared with subcutaneous adipose tissue. By measuring the gene expression levels of amino acid transporters in prostate cancer, our research group found that the transport mechanism of *trans*-1-amino-3-^{18}F-fluorocyclobutanecarboxylic acid involves not only system L but also system ASC [19]. Hence, gene analysis enables accurate determination of the detailed transport and uptake mechanism of radiotracers.

For in vivo studies, we selected H441 cells, which have high expression levels of all of the genes of system L and ASC, and PC14 cells, which display the lowest level of expression of system L and ASC genes of the four tumor lines assayed (Table 1). The transport mechanism of ^{14}C-L-MET and ^{3}H-D-MET in these cells that was identified in an in vitro study was confirmed in H441 and PC14-bearing mice (Table 2). As shown by the expression levels of the genes of the different transport systems, tumor accumulation of ^{14}C-L-MET and ^{3}H-D-MET was significantly higher in H441 than in PC14 cells, and in particular, accumulation of ^{3}H-D-MET was significantly increased (P<0.01). In PC14 cells, the accumulation of ^{3}H-D-MET was significantly lower than

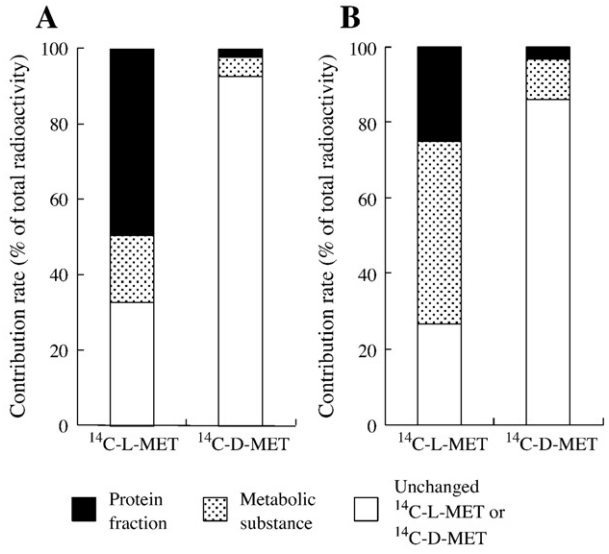

Fig. 4. Proportion of ^{14}C-L-MET and ^{14}C-D-MET incorporated into protein and nonprotein metabolites in liver and kidney of normal mice. The percentage of ^{14}C-L-MET and ^{14}C-D-MET incorporated into protein and nonprotein metabolites and the percentage of parent ^{14}C-L-MET and ^{14}C-D-MET in the liver (A) and kidney (B) were measured at 10 min after radiotracer injection. The combination of all three values was set at 100% for each organ. The incorporation of ^{14}C-D-MET into protein and nonprotein metabolites was lower than that of ^{14}C-L-MET, and over 80% of the ^{14}C-D-MET remained unmetabolized.

that of ^{14}C-L-MET ($P<0.01$). However, Bergström et al. [20] reported that the accumulation of ^{11}C-D-MET was lower than that of ^{11}C-L-MET in a brain tumor. These data suggest that if the transport systems involved in the transport of ^{3}H-D-MET are highly expressed in tumor cells, then tumor accumulation of ^{3}H-D-MET would be greater than that of ^{14}C-L-MET.

One of the reasons why ^{11}C-D-MET is useful in tumor diagnosis is that it is metabolically stable in plasma samples [10]. Therefore, in our study, we examined the incorporation of ^{14}C-L-MET and ^{14}C-D-MET, which have similar characteristics to ^{11}C-D-MET, into hepatic and liver proteins and nonprotein molecules, as well as the level of unincorporated ^{14}C-L-MET and ^{14}C-D-MET (Fig. 4). Approximately 25% to 40% of ^{14}C-L-MET was incorporated into protein, but the incorporation of ^{14}C-D-MET was significantly lower at approximately 3%. We also confirmed that more than 80% of ^{14}C-D-MET was unincorporated; in other words, ^{14}C-D-MET is not highly incorporated into proteins. There have been a few reports of large amounts of D-MET being converted into L-MET by D-amino acid oxidase via α-keto-γ-methiobutyrate, and of L-MET being utilized for protein synthesis [21,22]. However, in our study, only approximately 3% of ^{14}C-D-MET was utilized for protein synthesis (Fig. 4). We therefore predict that it is unlikely that metabolites of ^{14}C-D-MET would affect the accumulation of ^{14}C-D-MET in tumor cells. As shown in Table 2, the accumulation of ^{3}H-D-MET in the liver was lower than that of ^{14}C-L-MET. Both ^{14}C-L-MET and ^{3}H-D-MET accumulated in the pancreas, where amino acids are known to accumulate and protein synthesis is active, suggesting that both ^{14}C-L-MET and ^{3}H-D-MET are recognized as amino acids. ^{14}C-L-MET and ^{3}H-D-MET accumulated to the same degree in muscle. The accumulation of ^{3}H-D-MET was higher than that of ^{14}C-L-MET in plasma at early time points after injection, but it was subsequently rapidly cleared. As a consequence, the tumor-to-muscle ratio and the tumor-to-liver ratio of ^{3}H-D-MET were significantly increased compared with the ratios of ^{14}C-L-MET for both H441 and PC14 tumors. On the other hand, the tumor-to-plasma ratios of ^{14}C-L-MET were higher than those of ^{3}H-D-MET for up to 30 min after injection, whereas the reverse was the case at 60 min after injection, which is consistent with a report by Tsukada et al. [10]. Our results show that ^{11}C-D-MET, unlike ^{11}C-L-MET, is not incorporated into protein, has few metabolites and is accumulated in tumor cells via the specific neutral amino acid transport systems L and ASC. We speculate that other D-amino acid tumor imaging radiotracers may also be transported by a different transport mechanism from that of their L-amino acid.

5. Conclusion

The transport mechanism of ^{3}H-L-MET and ^{3}H-D-MET in human-derived tumor cells differed. ^{3}H-D-MET was transported by systems L and ASC, whereas ^{3}H-L-MET was transported by system L. In an in vivo study, tumor uptake and accumulation of ^{3}H-D-MET were significantly greater than that of ^{14}C-L-MET. Incorporation of ^{14}C-D-MET into protein and nonprotein molecules was significantly lower than that of ^{14}C-L-MET. Based on the above in vitro and in vivo studies, we conclude that ^{11}C-D-MET is a potentially useful radiotracer for tumor imaging in PET studies of metabolic organs.

References

[1] Kanai Y, Segawa H, Miyamoto K, Uchino H, Takeda E, Endou H. Expression cloning and characterization of a transporter for large neutral amino acids activated by heavy chain of 4F2 antigen (CD98). J Biol Chem 1998;273(37):23629–32.

[2] Bröer S. Amino acid transport across mammalian intestinal and renal epithelia. Physiol Rev 2008;88(1):249–86.

[3] Palacín M, Estévez R, Bertran J, Zorzano A. Molecular biology of mammalian plasma membrane amino acid transporters. Physiol Rev 1998;78(4):969–1054.

[4] Stern PH, Wallace CD, Hoffman RM. Altered methionine metabolism occurs in all members of a set of diverse human tumor cell lines. J Cell Physiol 1984;119(1):29–34.

[5] Kaschten B, Stevenaert A, Sadzot B, Deprez M, Degueldre C, Del Fiore G, et al. Preoperative evaluation of 54 gliomas by PET with fluorine-18-fluorodeoxyglucose and/or carbon-11-methionine. J Nucl Med 1998;39(5):778–85.

[6] Kim S, Chung JK, Im SH, Jeong JM, Lee DS, Kim DG, et al. ^{11}C-methionine PET as a prognostic marker in patients with glioma: comparison with ^{18}F-FDG PET. Eur J Nucl Med Mol Imaging 2005;32(1):52–9.

[7] Kubota K, Matsuzawa T, Fujiwara T, Ito M, Hatazawa J, Ishikawa K, et al. Differential diagnosis of lung tumor with positron emission tomography: a prospective study. J Nucl Med 1990;31(12):1927–32.

[8] Takeda A, Goto R, Tamemasa O, Chaney JE, Digenis GA. Biological evaluation of radiolabeled D-methionine as apparent compound in potential nuclear imaging. Radioisotopes 1984;33(4):213–7.

[9] Schober O, Duden C, Meyer GJ, Muller JA, Hundeshagen H. Non selective transport of [^{11}C-methyl]-L- and D-methionine into a malignant glioma. Eur J Nucl Med 1987;13(2):103–5.

[10] Tsukada H, Sato K, Fukumoto D, Nishiyama S, Harada N, Kakiuchi T. Evaluation of D-isomers of *O*-^{11}C-methyl tyrosine and *O*-^{18}F-fluoromethyl tyrosine as tumor-imaging agents in tumor-bearing mice: comparison with L- and D-^{11}C-methionine. J Nucl Med 2006;47(4):679–88.

[11] Shikano N, Kawai K, Nakajima S, Kubodera A, Kubota N, Ishikawa N, et al. Transcellular transport of radioiodinated 3-iodo-α-methyl-L-tyrosine across monolayers of kidney epithelial cell line LLC-PK$_1$. Ann Nucl Med 2004;18(3):227–34.

[12] Shotwell MA, Jaymes DW, Kilberg MS, Oxender DL. Neutral amino acid transport system in Chinese hamster ovary cells. J Biol Chem 1981;256(11):5422–7.

[13] Nakajima N, Shikano N, Kotani T, Ogura M, Nishii R, Yoshimoto M, et al. Pharmacokinetics of 3-[^{125}I]iodo-α-methyl-L-tyrosine, a tumor imaging agent, after probenecid loading in mice implanted with colon cancer DLD-1 cells. Nucl Med Biol 2007;34(8):1003–8.

[14] Oxender DL, Christensen HN. Distinct mediating system for the transport of natural amino acids. J Biol Chem 1963;238(11):3686–99.

[15] Guerino F, Baumrucker CR. Identification of methionine and lysine transport systems in cattle small intestine. J Anim Sci 1987;65(2):630–40.

[16] Shikano N, Nakajima S, Kotani T, Ogura M, Sagara J, Iwamura Y, et al. Transport of D-[1-^{14}C]-amino acid into Chinese hamster ovary (CHO-K1) cells: implications for use of labeled D-amino acids as molecular imaging agents. Nucl Med Biol 2007;34(6):659–65.

[17] Forstner C, Egberts J, Ammerpohl O, Niedzielska D, Buchert R, Mikecz P, et al. Gene expression patterns and tumor uptake of ^{18}F-FLT, and ^{18}F-FEC in PET/MRI of an orthotopic mouse xenotransplantation model of pancreatic cancer. J Nucl Med 2008;49(8):1362–70.

[18] Christen T, Sheikine Y, Rocha VZ, Hurwitz S, Goldfine AB, Di Carli M, et al. Increased glucose uptake in visceral versus subcutaneous adipose tissue revealed by PET imaging. JACC Cardiovasc Imaging 2010;3(8):843–51.

[19] Okudaira H, Shikano N, Nishii R, Miyagi T, Yoshimoto M, Kobayashi M, et al. Putative transport mechanism and intracellular fate of trans-1-amino-3-^{18}F-fluorocyclobutanecarboxylic acid in human prostate cancer. J Nucl Med 2011;52(5):822–9.

[20] Bergström M, Lundqvist H, Ericson K, Lilia A, Johanström P, Långström B, et al. Comparison of the accumulation kinetics of L-(methyl-^{11}C)-methionine and D-(methyl-^{11}C)-methionine in brain tumors studies with positron emission tomography. Acta Radiol 1987;28(3):225–9.

[21] Berg CP. Physiology of the D-amino acids. Physiol Rev 1953;33(2):145–89.

[22] Stegink LD, Moss J, Printen KJ, Cho ES. D-methionine utilization in adult monkeys fed diets containing DL-methionine. J Nutr 1980;110(6):1240–6.